Research article

Ecology Journal

ISSN (Print): 2957-4471, ISSN (Online): 2957-448X, Website: https://journal.esbangladesh.org
Ecol. J. (2025) 7 (3) : 211-225

Spatiotemporal assessment on above-ground biomass and carbon stock dynamics in Bhawal National Park of Bangladesh using GEDI LiDAR and Sentinel-2 Data

Mumtahina Akter[1], Asib Ahmed[1*] and Md. Toriqul Islam[2]

[1]Department of Geography and Environment, University of Dhaka, Bangladesh; [2]NGO Forum for Public Health, Dhaka, Bangladesh.

***Corresponding e-mail:** asib01geo@du.ac.bd

Received: 09 October 2025, revised: 28 November 2025, accepted: 30 November 2025, DOI: https: //doi.org/10.59619/ej.7.3.5

Abstract

Forests are essential for regulating the global climate and carbon balance. Monitoring Above-ground Biomass (AGB) and its Density (AGBD) at high resolution is needed for sustainable forest management, biodiversity conservation, and carbon accounting to support climate change mitigation. The present study aimed to assess the spatiotemporal changes in above-ground biomass (AGB) and carbon stock in Bhawal National Park (BNP) between 2019 and 2024. This involved integrating data from the Global Ecosystem Dynamics Investigation (GEDI) and Sentinel-2. A Random Forest (RF) regression model was applied to estimate AGB by combining the GEDI Level 4A footprint data with spectral and topographic variables derived from Sentinel-2 and digital elevation model (DEM). The model showed good predictive performance, with R^2 values above 0.80 for both years. The results revealed a significant decline in total AGB from 355,242.50 Mg in 2019 to 307,035.78 Mg in 2024, corresponding to a carbon stock loss of 22,657.16 Mg. Spatial analysis showed that high-biomass zones have shrunk, while low and moderate-biomass areas have expanded, especially along forest edges and in degraded areas. Field validation confirmed a moderate match between estimated and observed AGB values. The study identified deforestation, land-use change, and fragmentation as the main drivers of biomass decline. These findings highlight ongoing forest degradation in one of Bangladesh's most important Sal forest ecosystems. This emphasizes the urgent need for improved forest monitoring and conservation strategies. Integrating GEDI and optical satellite data offers a cost-effective approach for large-scale forest assessment, supporting national carbon accounting, REDD+ implementation, and sustainable forest management.

Keywords: Above-ground biomass, carbon, GEDI LiDAR, Sentinel-2, forest

Introduction

Forests are essential components of the Earth's biosphere, playing a crucial role in climate regulation through the sequestration and storage of atmospheric carbon. Globally, forest ecosystems store about 80% of terrestrial carbon, with approximately 50% of their total biomass composed of carbon (Pan *et al.* 2011, Nuthammachot *et al.* 2020). The quantification of above-ground biomass (AGB), the total dry mass of living vegetation above the soil, including stems, branches, bark, and leaves, is therefore central to understanding the carbon dynamics of forest ecosystems. Above-ground carbon (AGC) is usually calculated as about 47–50% of above-ground biomass (AGB). It is a key indicator for assessing an ecosystem's capacity to act as a carbon sink and for evaluating its contribution to global carbon balance (IPCC 2006, Chave *et al.* 2014).

Accurate estimation of forest AGB and carbon stock is essential for carbon accounting, forest management, and climate mitigation programs such as REDD+. High-resolution, spatio-temporally estimates of AGB and AGBD are crucial for precise carbon accounting and informed ecosystem management decisions (Friedlingstein *et al.* 2025, Pan *et al.* 2011). Traditional field-based inventory methods are reliable at local scales but are time-consuming, labor-intensive, and limited in spatial coverage. Although in situ measurements of AGBD provide the highest accuracy, satellite remote sensing has become the main method for large-scale biomass estimation, because of its wide coverage and operational efficiency (Chamberlin *et al.* 2025, Lu *et al.* 2006). The integration of remote sensing technologies, particularly LiDAR (Light Detection and Ranging), has transformed biomass estimation by providing detailed vertical structure information over large areas (Lu 2006, Dubayah *et al.* 2020).

The Global Ecosystem Dynamics Investigation (GEDI), launched by NASA in 2018 aboard the International Space Station, represents a major advancement in this field. GEDI provides high-resolution, waveform LiDAR data capable of capturing forest canopy height, vertical structure, and above-ground biomass density (AGBD) at the global scale (Dubayah *et al.* 2020). Its Level 4A (L4A) product delivers footprint-level AGB estimates (~25 m), generated through regression models calibrated with field and airborne LiDAR data (Duncanson *et al.* 2022). This dataset enables a more consistent, fine-scale assessment of forest biomass change than traditional optical sensors, which often suffer from signal saturation in dense canopies (Zhang & Ni-Meister 2014).

The forest areas of Bangladesh, particularly the Sal (Shorea robusta) forests of Bhawal National Park (BNP), are under severe anthropogenic pressure from industrial expansion, agricultural encroachment, and settlement growth. Once a biologically rich ecosystem, BNP has experienced substantial deforestation and degradation over the last two decades, leading to a notable decline in forest biomass and associated carbon storage (Rahman *et al.* 2023). Despite its ecological significance, no studies were found that analyzed the spatiotemporal dynamics of biomass and carbon stock in this protected area using advanced spaceborne LiDAR data.

Given this gap, the present study employs GEDI L4A data integrated with Sentinel-2 and topographic variables to estimate and analyze AGB and carbon stock changes in Bhawal National Park between 2019 and 2024. The specific objectives are to (i) map the spatial distribution of AGB for the years 2019 and 2024 using Random Forest regression; (ii) quantify the temporal variation in AGB and carbon stock; and (iii) validate GEDI-derived biomass estimates with field measurements. By utilizing GEDI's high-resolution data, this study provides a robust assessment of biomass decline and carbon loss in one of Bangladesh's most threatened forest ecosystems. The findings offer valuable insights for REDD+ implementation and sustainable forest conservation.

Materials and methods

Study area: Bhawal National Forest is located between 24°01′ to 24°11′ N latitude and 90°20′ to 90°28′ E longitude, within Gazipur District, approximately 40 km north of Dhaka (Fig. 1). This is one of Bangladesh's most ecologically and historically significant, as well as vulnerable, forests. It was declared a National Park

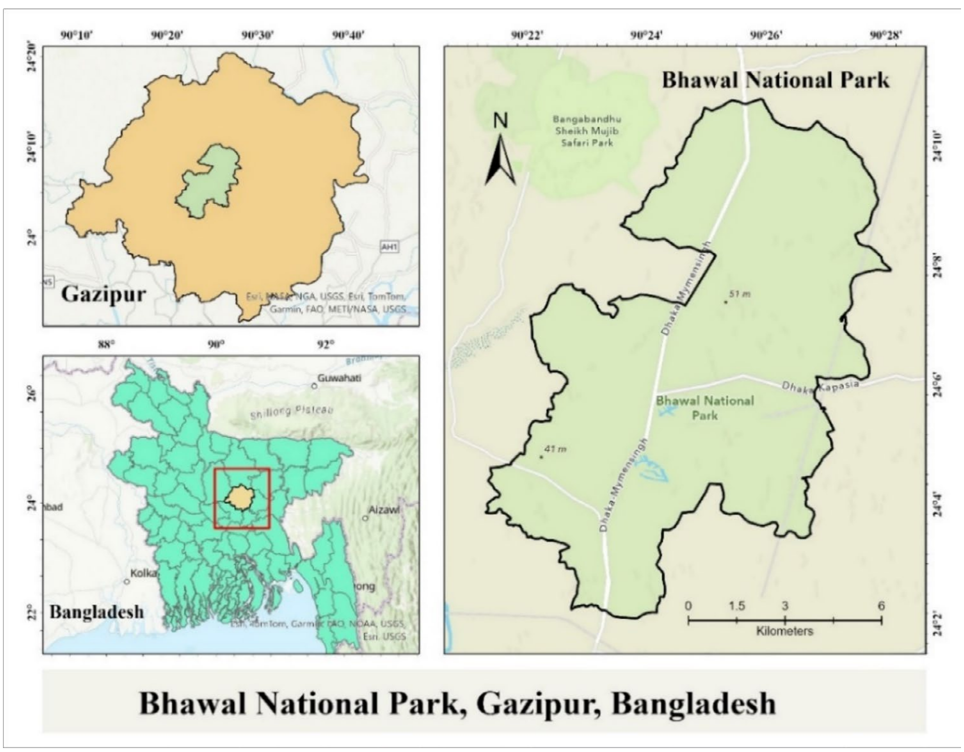

Figure 1. The geographical location of the study area.

Table 1. Overview of datasets and derived variables used for AGB estimation

Sentinel-2 band reflectance	Sentinel-2 derived vegetation indices	Digital Elevation Model (DEM)	GEDI Dataset
Band 1 (Aerosols), Band 2 (Blue),	NDVI		
Band 3 Green), Band 4 (Red), Band 5	MNDWI	Elevation	GEDI L4A
(Red edge 1), Band 6 (Red edge 2),	NDBI	Slope	AGBD
Band 7 (Red edge 3), Band 8 (Near Infrared),	EVI		Product
Band 8A (Near Infrared), B11 (Shortwave	BSI		
Infrared), B12 (Shortwave Infrared)			

in 1982 under the Bangladesh Wildlife (Preservation) Order 1974 (Kabir & Ahmed, 2005). The forest has been classified under IUCN Category IV, aiming to preserve habitat and species through active management. This site was selected due to its rich biodiversity, critical ecosystem services, and growing pressure from industrial expansion, illegal settlement, and land degradation. Bhawal National Park covered 5,022 ha; however, unpublished Forest Department data indicate that the two forest ranges that comprise the national park cover over 10,000 ha. For management purposes, Bhawal is divided into two zones: a core zone and a buffer zone. The core zone of about 950 ha is the area where protective measures are taken, and here conversion to industrial use, the extraction of forest products, and the planting of exotic species are supposed to be prohibited. (Jahan et al., 2017).

Data sources and preprocessing: This study used multi-source satellite data to estimate and analyze above-ground biomass (AGB) and carbon stock for the years 2019 and 2024 (Table 1). GEDI Level 4A footprint data were used as reference AGB values, while spectral indices derived from Sentinel-2 imagery served as predictor variables. For each year, cloud-masked Sentinel-2 surface reflectance collections were aggregated into annual median composites (January–December). From these composites, vegetation and water indices were calculated. The use of annual medians minimized the effects of seasonal variability and atmospheric noise, providing robust predictors for structural biomass estimation in a deciduous forest context.

Sentinel-2 surface reflectance: For predictor variables, Sentinel-2 Level-2A surface reflectance data were utilized. Sentinel-2 offers high-resolution multispectral imagery (10–20 m) across 13 bands, which are widely used for vegetation structure and biomass modeling (Delegido et al., 2011). Multispectral imagery from Sentinel-2 was used to derive key vegetation indices, which, along with original reflectance bands, served as independent variables. Sentinel-2 Level-2A surface reflectance images for the target year were processed in Google Earth Engine (GEE). A median composite was generated over the study period after applying cloud and shadow masking using the Sentinel-2 CloudScore+ algorithm. Several vegetation indices were computed from the spectral bands, including the Normalized Difference Vegetation Index (NDVI), Enhanced Vegetation Index (EVI), Modified Normalized Difference Water Index (MNDWI), and Bare Soil Index (BSI). These indices were selected due to their known relationships with vegetation cover and canopy biomass (Xie et al., 2018).

GEDI data: The primary dataset used for estimating above-ground biomass (AGB) was the Global Ecosystem Dynamics Investigation (GEDI) Level 4A (L4A) Aboveground Biomass Density (AGBD) product. The GEDI mission, launched by NASA in 2018 aboard the International Space Station, provides footprint-level biomass estimates with a spatial footprint of approximately 25 m (Dubayah et al., 2020). Each footprint contains AGB values (in Mg/ha). The raw GEDI L4A footprints were filtered to ensure data reliability. All measurements with l4_quality_flag = 0 or degrade_flag > 0 were removed to

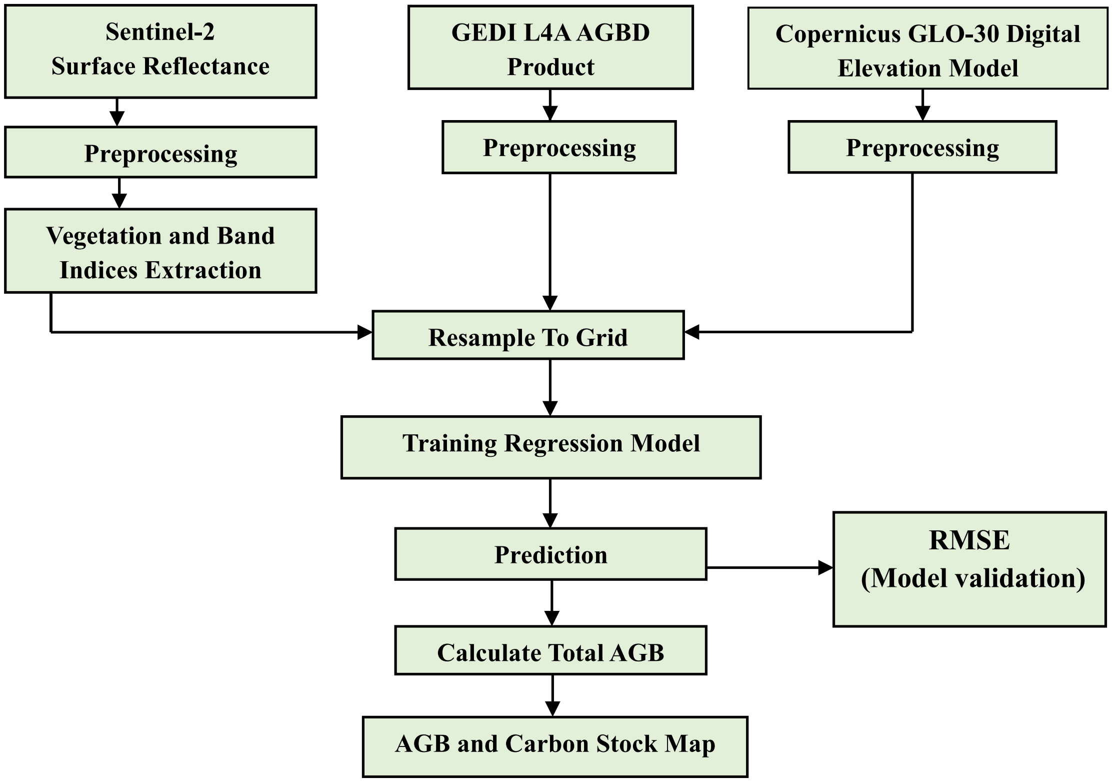

Figure 2. Methodological flow chart showing the data sources, analytical procedures, and final output.

ensure data quality. Footprints with degraded waveforms or high relative uncertainty (agbd_se/agbd > 0.5) were also excluded. Additionally, footprints on steep terrain (slope > 30°) were removed using the slope layer derived from GLO-30 DEM, as steep slopes can introduce errors in LiDAR backscatter and biomass estimates (Gandhi,2024).

Copernicus GLO-30 digital elevation model (DEM): Topographic variables, elevation, and slope were derived from the Copernicus GLO-30 Digital Elevation Model (DEM), which provides a 30 m resolution elevation layer globally. It was included as an additional predictor variable.

Estimating above-ground biomass: The AGB estimation method used in this study was adapted from the workflow developed by Gandhi (2024). This method integrated GEDI L4A AGB density with Sentinel-2 spectral data and elevation metrics within the Google Earth Engine (GEE) platform. This approach used a Random Forest regression model to predict AGB values across the study area by training on GEDI footprint data and a suite of vegetation and terrain predictors. The method allows for spatially explicit AGB mapping and can be widely applied in various ecosystems for estimating biomass and detecting forest degradation. Following this methodology, we generated AGB maps for the years 2019 and 2024, and derived total AGB values and RMSE to assess changes over time. Figure 2 shows the detailed methodology of the study, which involves field data collection, mapping the vegetation indices extraction, training the regression model, total AGB calculation, and model validation.

The Sentinel-2 composite and DEM layers were stacked to create a multi-band predictor dataset. The GEDI footprint data were then sampled to extract corresponding pixel values of the spectral and topographic variables. To harmonize resolutions and reduce computational load, all predictor layers were aggregated and resampled to a 100 m grid using the reduce resolution function in GEE with mean aggregation. The resampled dataset was then clipped to the study area boundary.

Building a regression model: A Random Forest (RF) regression model was applied to establish the relationship between GEDI-derived AGB values and the predictor variables. RF, a non-parametric ensemble learning algorithm, is known for its robustness against overfitting and ability to model complex, non-linear relationships between spectral data and biomass (Breiman, 2001). The model was implemented using GEE's Random Forest classifier with the number of 50 decision trees. The GEDI AGBD values served as the dependent variable (target), while Sentinel-2 bands, vegetation indices, and DEM-derived variables were used as independent predictors. 312 samples for 2024 and 169 samples for 2019 were extracted using a stratified random sampling strategy, ensuring balanced coverage of different biomass classes. The dataset was split into 70% training and 30% validation sets.

Model evaluation: The performance of the RF regression was evaluated using the Root Mean Square Error (RMSE). The coefficient of determination (R^2) between observed (GEDI) and predicted AGB values:

$$RMSE = \sqrt{\frac{1}{n}\sum_{i=1}^{n}\left(AGB_{\text{predicted},i} - AGB_{\text{observed},i}\right)^2}$$

The model's accuracy metrics were derived using the validation dataset and out-of-bag (OOB) estimates inherent to the RF algorithm.

Estimation of total biomass: The validated RF model was applied to the full predictor stack (Sentinel-2 and DEM layers) to generate a spatially continuous AGB map for the study area. Non-vegetated classes were masked out using the land use land cover map by retaining only vegetated land cover classes. The total AGB was calculated by multiplying the predicted AGB values (Mg/ha) by the pixel area (in hectares) and summing the values over the study area

$$AGB_{total} = \sum_{i=1}^{n}\left(AGB_i \times A_{pixel}\right)$$

Where AGB_i is the biomass (Mg/ha) of pixel i, and A_{pixel} is the area of a single pixel in hectares.

Validation with field plot data: Field data were collected to provide ground truth information for biomass estimation and to support the accuracy of the GEDI-derived AGB estimates. The forest map of the study area was initially derived from the land use and land cover classification of Sentinel-2 imagery for the year 2024. Based on this map, a total of 10 field sampling plots were randomly selected.

Each plot measured 10 m × 10 m (100 m^2), with boundaries physically delineated in the field using measuring tape. The geographic coordinates of the selected plots were used to locate them on the ground with the aid of a smartphone GPS. DBH was measured using a measuring tape, while tree height was measured using a Mileseey PF3S 1500M Laser Rangefinder. These values were input into standard allometric equations to calculate AGB per tree. The equation used was based on Chave et al. (2005), suitable for tropical forest ecosystems Muhe and Argaw (2022).

$$\mathbf{AGB = 0.0673 \times (\rho D^2 H)^{0.97}}$$

where AGB is aboveground biomass (kg), ρ is the wood density (g/cm^3), D is the DBH (cm), and H is the tree height (m). Species-specific wood density values were sourced from recognized global databases (Zanne et al, 2009).

The calculations were performed in Excel to obtain total AGB per plot in kilograms, which were then converted to megagrams per hectare (Mg/ha) by adjusting for the 0.01 ha plot size. These field-derived AGB values were compared with GEDI L4A AGB estimates extracted for corresponding plot locations. The comparison allowed for evaluation of the GEDI data's accuracy in estimating biomass at local scales.

Estimation of total carbon amount from AGB: To estimate the total carbon content in the study area, the aboveground biomass (AGB) values were converted to carbon stock using a standard conversion factor. Following Intergovernmental Panel on Climate Change (IPCC) guidelines, a carbon fraction (CF) of 0.47 was applied to AGB estimates. The equation used was:

Total carbon (Mg C/ha) =AGB (Mg/ha) × CF

This conversion was performed only for the current year (2025) to estimate the present state of carbon sequestration in the study area. The carbon stock map generated from this calculation provides a spatial representation of ecosystem carbon storage. Subsequently, it was analyzed in the context of recent forest cover status and biomass distribution. This approach gives a clear picture of the carbon storage potential based on the most recent land cover and biomass data.

Results

Estimating above-ground biomass (AGB) and carbon stock was conducted using regression modeling based on GEDI LiDAR-derived AGBD data. The results, summarized in Table 2, show a consistent declining trend in both total biomass and carbon stock between 2019 and 2024. In 2019, the total AGB was estimated at 355,242.50 Mg, which decreased to 307,035.78 Mg in 2024. The corresponding carbon stock declined from 166,963.98 Mg to 144,306.81 Mg. The model performance was strong for both years, with R^2 values of 0.805 and 0.804 and RMSE values of 19.25 Mg/ha and 21.74 Mg/ha, respectively, indicating good predictive accuracy and stable model reliability across years.

The scatter plots (Fig. 3) show the relationship between predicted and observed AGB values derived from the GEDI L4A dataset. Both years exhibited strong positive correlations, confirming the model's robustness in predicting biomass. However, a slight dispersion is visible in the 2024 plot, reflected by the slightly higher RMSE value, which suggests minor underestimation in areas with higher observed biomass.

The mean AGB values derived from GEDI L4A AGBD data were 82.44 Mg/ha in 2019 and 79.76 Mg/ha in 2024. This decline of approximately 2.68 Mg/ha indicates a

Table 2. Estimated total above-ground biomass (AGB) and carbon stock (2019–2024)

Year	Total AGB (Mg)	Carbon Stock (Mg)	R^2	RMSE (Mg/ha)
2019	355242.502	166963.975	0.805	19.249
2024	307035.775	144,306.814	0.804	21.738

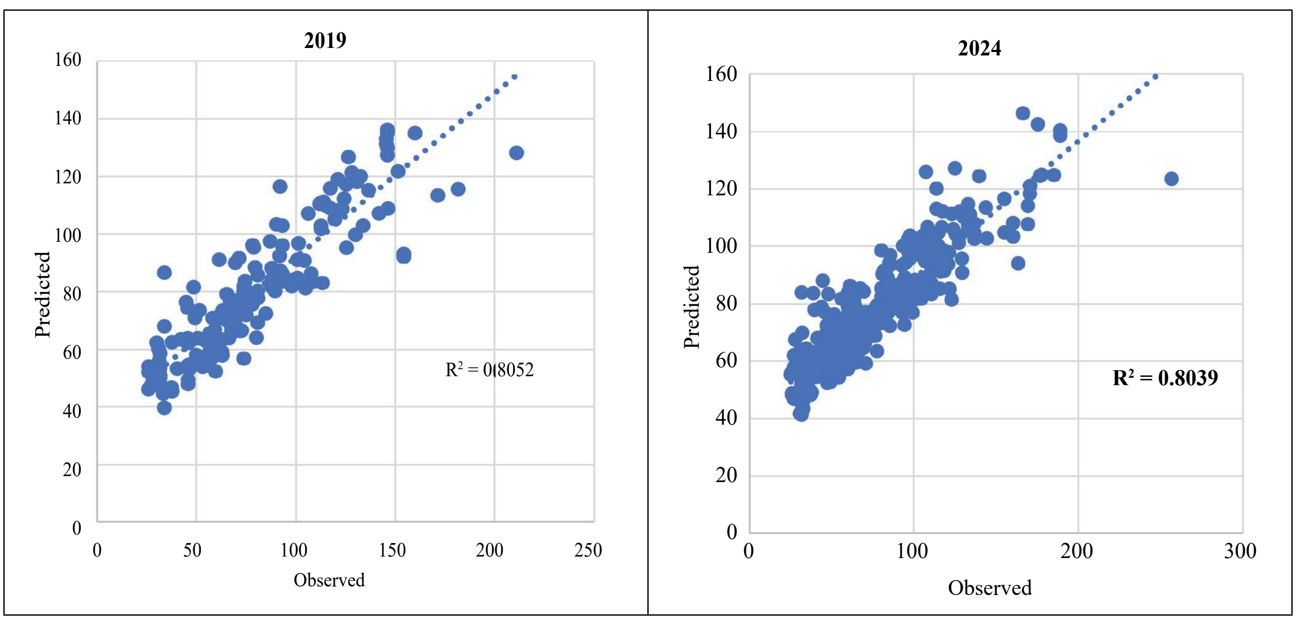

Figure 3. Scatter plots showing regression relationships between GEDI-observed and model-predicted AGB values for the years 2019 and 2024, indicating model accuracy (R^2 and RMSE).

gradual reduction in biomass density, consistent with the total biomass loss observed at the landscape scale. These results collectively demonstrate that Bhawal National Park has experienced both spatial and quantitative declines in biomass over the five years.

The spatial distribution of AGB (Fig. 4) further illustrates these changes. In 2019, high AGB zones were concentrated in the central and eastern regions of the park, particularly within the dense forest cores. By 2024, these high-biomass areas had visibly contracted, replaced by larger zones of low to moderate AGB, particularly along the forest periphery. This pattern reflects the ongoing processes of forest degradation and canopy thinning within the park. Similarly, the carbon stock maps (Fig. 5) show a similar spatial pattern. Higher carbon density areas correspond closely with the zones of high AGB, while

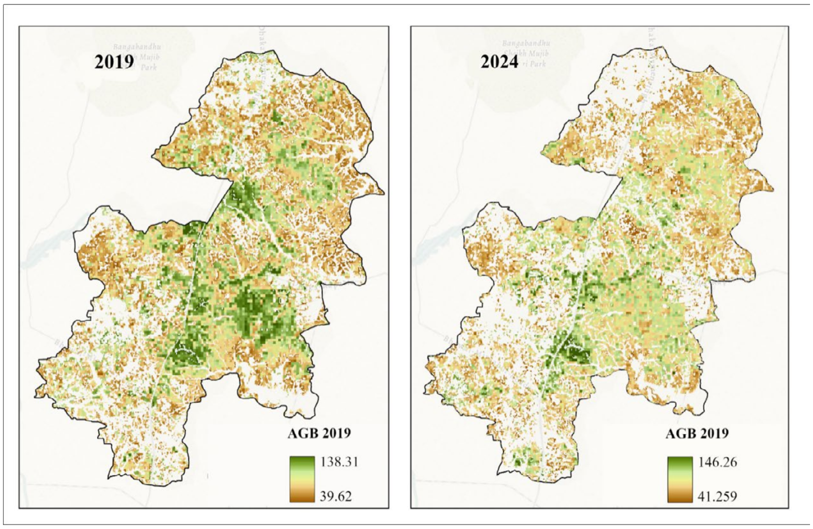

Figure 4. Spatial distribution of above-ground biomass (AGB) in 2019 and 2024. AGB maps showing biomass density variation across Bhawal National Park, with darker tones indicating higher AGB density and lighter tones indicating lower biomass.

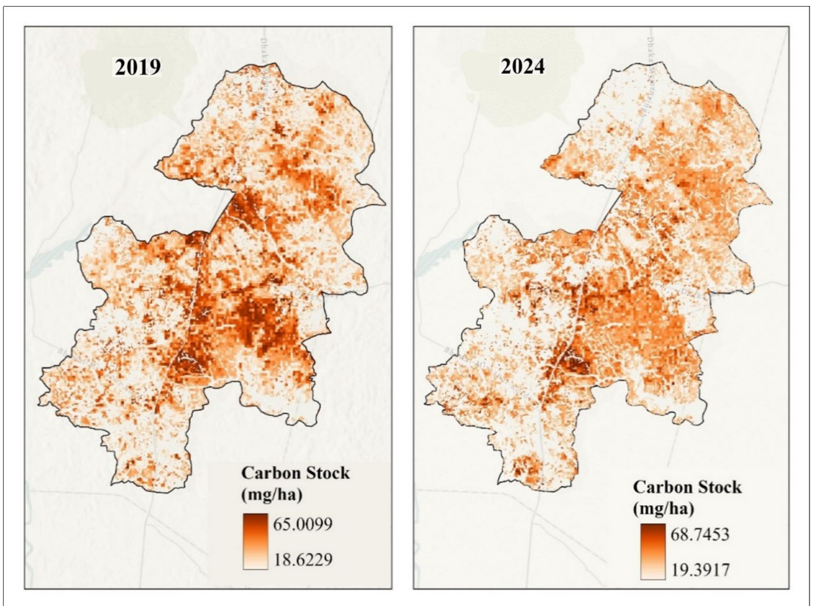

Figure 5. Carbon stock distribution in the study area for 2019 and 2024, derived from GEDI-based above-ground biomass estimates.

regions showing reduced biomass also display lower carbon storage capacity. The spatial overlap between declining biomass and carbon stock suggests that forest degradation is directly responsible for reduced carbon sequestration potential.

Validation of GEDI-Derived AGB with field measurement: To evaluate the predictive accuracy of GEDI-derived AGB, 10 ground plots (10 m × 10 m) were sampled in 2025 for field-based biomass measurements. These measurements were then compared with GEDI-predicted AGB values for 2024 (Table 3).

The validation of GEDI-derived AGB predictions against 2025 field data revealed a generally moderate level of agreement. Particularly in plots with average biomass density ranging between 100 and 150 Mg/ha. The predicted AGB values remain relatively stable across all plots, ranging between 70 and 140 Mg/ha. In contrast, observed AGB shows high variability, fluctuating sharply between ~50 Mg/ha and ~257 Mg/ha.

Discussion

Decreasing AGB and Carbon Stock trends: The analysis of GEDI-derived AGB from 2019 to 2024 reveals a steady and significant decline in above-ground biomass and carbon stock within Bhawal National Park. Over these five years, total AGB decreased by approximately 48,206 Mg, equivalent to a carbon loss of nearly 22,657 Mg. The average AGB density also showed a consistent downward trend, indicating widespread degradation even within areas classified as forest. This trend aligns with national-level observations. A recent study by Mojumder *et al.* (2023) reported a decline in average AGB in Bangladesh's Madhupur Sal Forest, from 110.01 Mg/ha in 2014 to 107.22 Mg/ha in 2020. The loss was caused by illegal felling, encroachment, shifting cultivation, and urban expansion. Similarly, significant AGB loss was found in the Nijhum Dwip mangrove forest, which declined by 16% over the same period. These patterns reflect broader national concerns, as Bangladesh faces one of the highest rates of deforestation in South Asia, losing around 2,600 ha of forest annually, primarily due to human pressure (FAO, 2015; Rahman *et al.*, 2023). The declining trend in AGB and carbon stock signifies not only a reduction in forest biomass but also a decrease in carbon sequestration capacity, undermining the park's role as a carbon sink. This pattern corresponds with global findings where tropical forests are gradually losing their net carbon sink function due to deforestation and degradation (Harris *et al.*, 2021). GEDI-based estimates provide more reliable structural measurements than optical sensors. The temporal consistency of the decline across all observation years reinforces the evidence of continuous ecosystem degradation rather than data-related variability.

Table 3. Validation of GEDI-Derived AGB (2024) with Field Measurements (2025)

Plot No	Field data (2025) (Mg/ha)	Predicted from GEDI (2024) (Mg/ha)
Plot 1	136.237	125.715
Plot 2	192.019	146.267
Plot 3	42.200	63.505
Plot 4	257.713	59.390
Plot 5	177.530	120.147
Plot 6	158.472	108.574
Plot 7	79.361	76.334
Plot 8	191.709	101.119
Plot 9	144.2135	105.135
Plot 10	138.661	104.145

Changes in spatial patterns of AGB: The spatial analysis of AGB dynamics between 2019 and 2024 revealed significant biomass loss and low biomass gain across the study area (shown in Figure 6). The values range from (–63.15 to +67.44) Mg/ha, where positive values denote biomass gain and negative values indicate biomass loss. While patches of biomass gain (green areas) likely indicate natural forest regeneration, secondary succession, or localized afforestation, the widespread zones of biomass loss (red and orange areas), particularly in the core and southern regions, suggest ongoing forest degradation.

This degradation may occur due to selective anthropogenic disturbances such as logging, settlement expansion, and industrial activities. The green zones indicate biomass

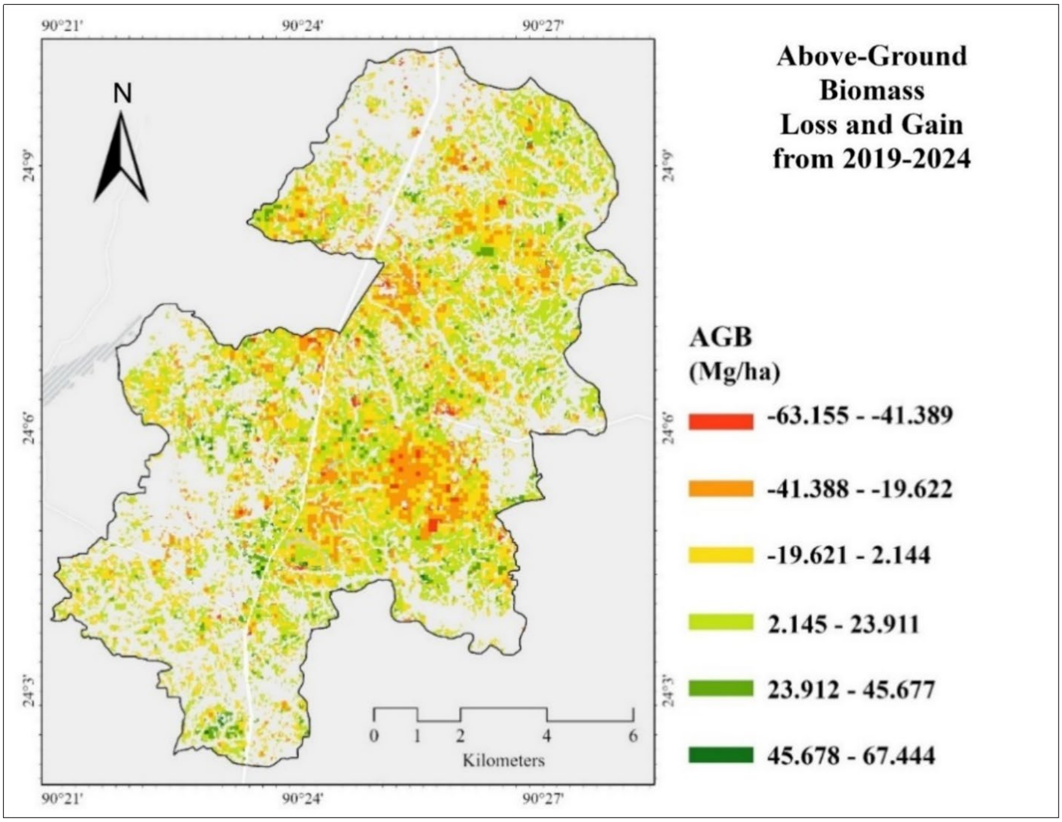

Figure 6. Spatial distribution of above-ground biomass (AGB) change in the study area between 2019 and 2024, showing zones of biomass loss (red to yellow) and biomass gain (light to dark green). Negative values indicate biomass reduction due to forest degradation or anthropogenic activities, while positive values represent biomass accumulation from natural regeneration or reforestation efforts.

gain, likely due to natural regeneration or reformation efforts. The majority of the study area is characterized by yellow and orange tones, indicating mild to moderate biomass loss, with only a few patches exhibiting significant biomass gain.

Decline of above-ground biomass (AGB) density between 2019 and 2024: Based on the AGB maps (shown in Figure 7) for 2019 and 2024, five distinct biomass classes were identified, ranging from very low to very high density. In 2019, very low AGB density (39.62–59.36 Mg/ha) and low density (59.36–79.10 Mg/ha) zones were mainly distributed along the outer and fragmented forest edges, while moderate density (79.10–98.84 Mg/ha) covered transitional forest areas. The high (98.84–118.58 Mg/ha) and very high density (118.58–138.31 Mg/ha) classes were concentrated in the central and southern regions (Rajendrapur forest beat, representing dense forest stands.

By 2024, a notable reduction is observed in the high and very high-density areas, with an expansion of the low and moderate density classes (41.26–104.26 Mg/ha), particularly in the northern and eastern parts. This shift indicates a significant decline in above-ground biomass, likely resulting from forest cover loss, degradation, and fragmentation. The reduction of dense forest zones corresponds with anthropogenic pressures such as deforestation, illegal logging, and land-use conversion. These activities ultimately lead to decreased biomass and carbon stock potential in the region.

Possible causes of AGB and carbon stock loss: The reduction of above-ground biomass (AGB) and carbon stock observed between 2019 and 2024 in Bhawal National

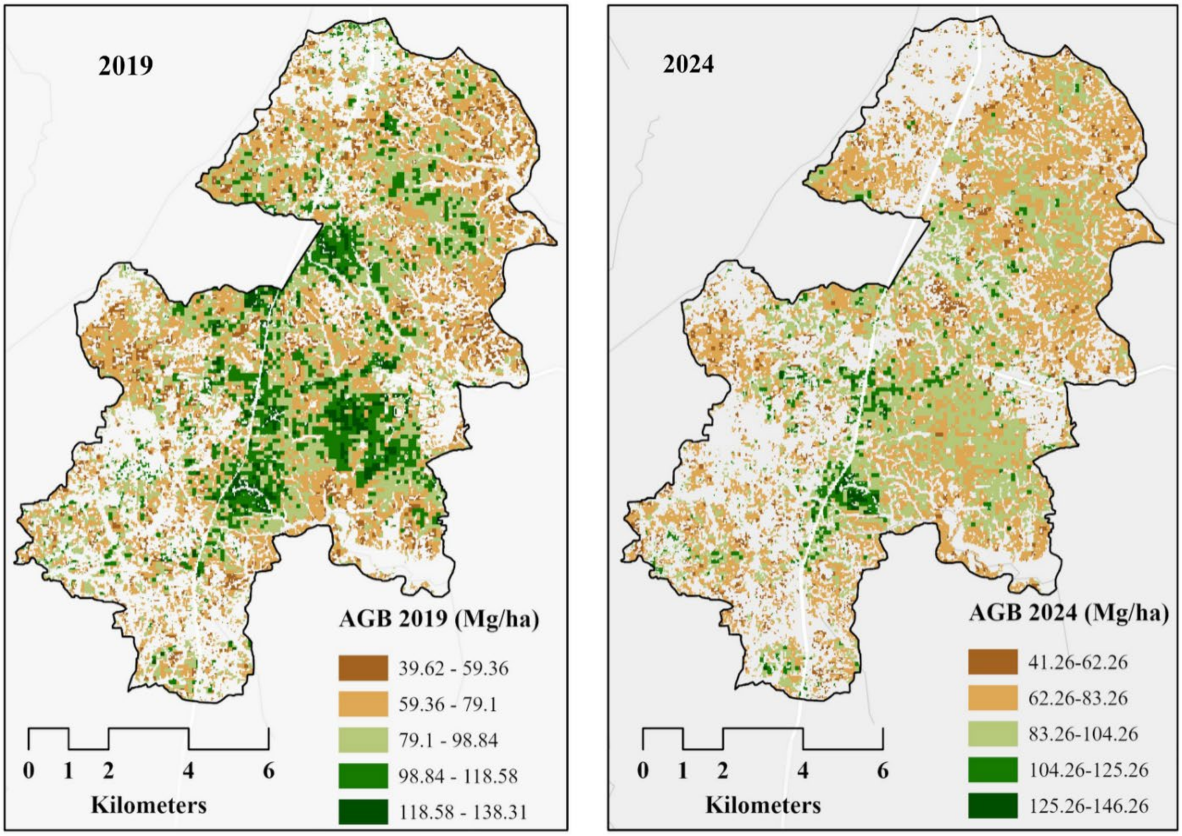

Figure 7. Classification of above ground biomass (AGB) density (2019 vs 2024), comparative visualization of AGB density classes (very low to very high) in 2019 and 2024, highlighting a reduction in high-density forest zones.

Park is closely linked to three interrelated processes. These are forest cover loss, forest degradation, and fragmentation. Each process contributes to a measurable decline in the park's biomass density and overall carbon sequestration capacity.

Forest cover loss: The land use and land cover (LULC) analysis revealed that total forest area in Bhawal National Park declined from 5,725.28 ha in 2019 to 5,365.94 ha in 2024, representing a loss of approximately 359.34 ha (6.28%) over five years (Fig. 8). This contraction in forest extent directly translates to a decrease in the total area capable of storing biomass and carbon.

The reduction primarily occurred along the park's southern and eastern boundaries, where industrial and settlement expansion have been most intense. High-resolution satellite imagery confirmed the conversion of forest patches into built-up and agricultural land, reflecting a clear pattern of deforestation. Similar findings have been reported in other Salforest ecosystems of Bangladesh, where unregulated land conversion has led to continuous carbon stock depletion (Islam et al., 2017; Rahman et al., 2023). The forest cover loss observed here not only eliminates mature tree stands but also reduces canopy connectivity, accelerating soil erosion and altering microclimatic conditions that hinder natural regeneration. Consequently, forest loss remains the dominant driver of AGB and carbon decline during the study period.

Forest degradation: Even within remaining forested zones, AGB density showed a marked reduction, suggesting widespread forest degradation rather than complete clearance (Fig. 9). GEDI-derived biomass estimates revealed declining canopy height and structure, indicating canopy thinning, selective logging, and

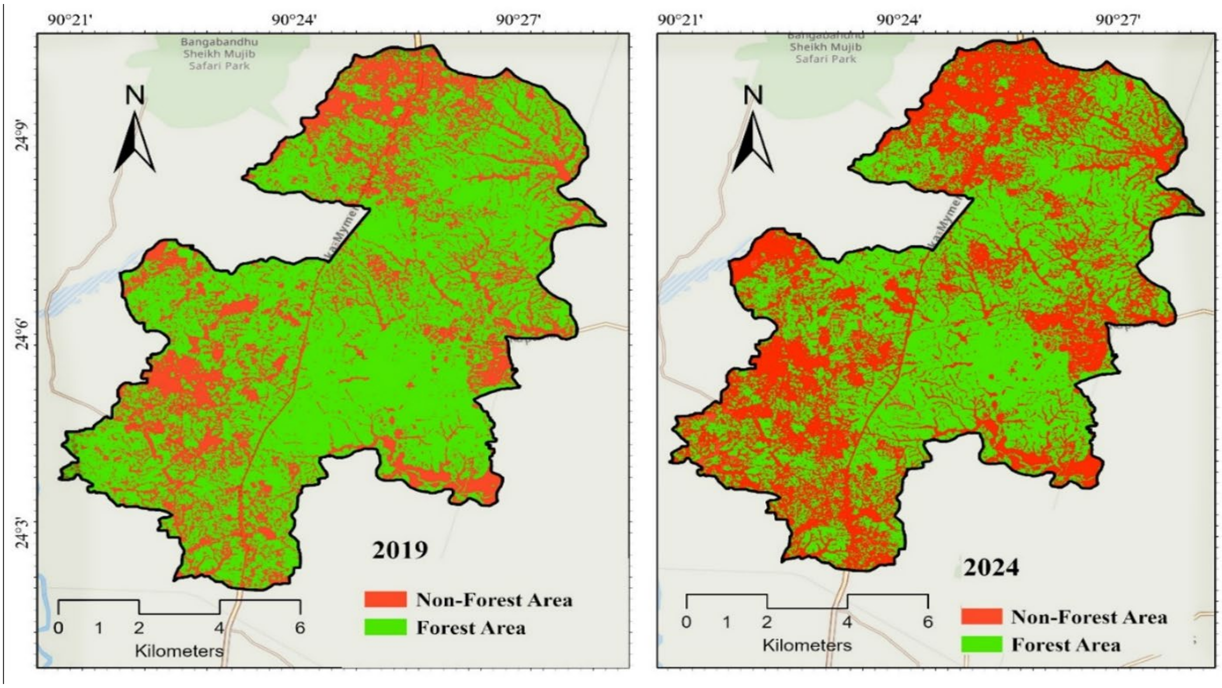

Figure 8. Map showing forest and non-forest cover of 2019 and 2024.

understory clearing. These subtle forms of degradation are often undetected in conventional satellite imagery but have significant implications for carbon storage. As forests degrade, the amount of living plant material shrinks, and deadwood piles up. Over time, the dead wood decays and releases the stored carbon back into the soil or the atmosphere Wijas et al. 2024; Błońska et al. 2019.

In Bhawal National Park, local communities depend on forest resources for fuelwood, grazing, and small-scale timber extraction. While these activities do not fully remove forest cover, they collectively reduce stand density and tree maturity, lowering per-hectare biomass.

Forest fragmentation: The spatial configuration of forest patches has also changed significantly between 2019 and 2024, with fragmentation emerging as a key contributor to biomass loss. Continuous forest blocks have become increasingly divided by agricultural plots, roads, and settlements, creating numerous edge habitats with reduced biomass density (Fig. 10). Fragmentation intensifies exposure to edge effects such as increased sunlight, wind stress, and human disturbance, all of which reduce tree growth and survival.

The Random Forest regression model revealed that biomass density tends to be lower near forest edges and access routes, confirming the spatial influence of fragmentation on AGB decline. Fragmentation also limits natural regeneration by isolating forest patches and reducing seed dispersal, leading to long-term declines in carbon accumulation capacity.

Validation results- correlation between GEDI and field data: The validation of GEDI-derived AGB predictions against field data reveals a generally moderate level of agreement, particularly in plots with average biomass density. Figure 11 presents a comparative assessment of observed versus predicted above-ground biomass (AGB) across 10 field plots within the study area. The observed AGB values, obtained from field measurements, are consistently higher than the predicted values generated from the regression model, particularly in plots with high biomass density.

The most significant dissimilarity is evident in Plot 4, where the observed AGB exceeds 250 Mg/ha, while the predicted value remains below 100 Mg/ha. This divergence is primarily attributed to the unique characteristics of Plot 4, which is situated in an urban

Figure 9. Forest degradation zones in Bhawal National Park. High-resolution satellite reveals forest degradation (marked in red box), canopy thinning, and forest fragmentation. (Source: Google Earth).

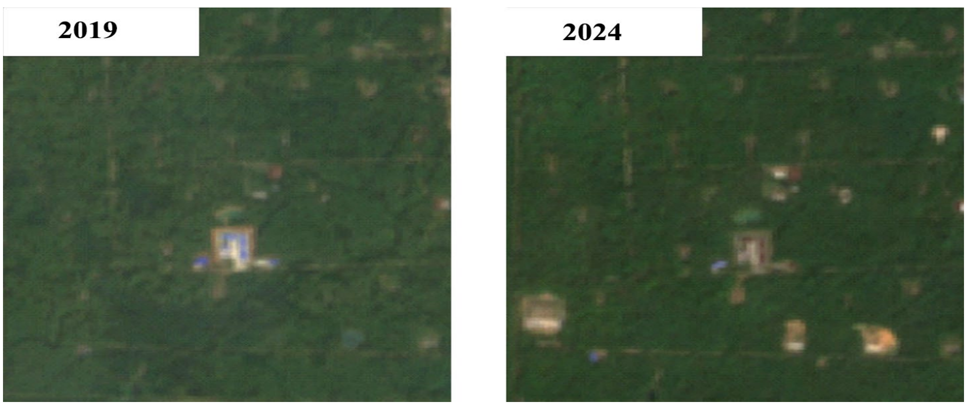

Figure 10. Forest fragmentation pattern in Bhawal National Park (2019–2024). Satellite images displaying increased forest fragmentation, showing isolated forest patches and edge expansion due to land-use conversion. (Source: Google Earth Engine, 2025).

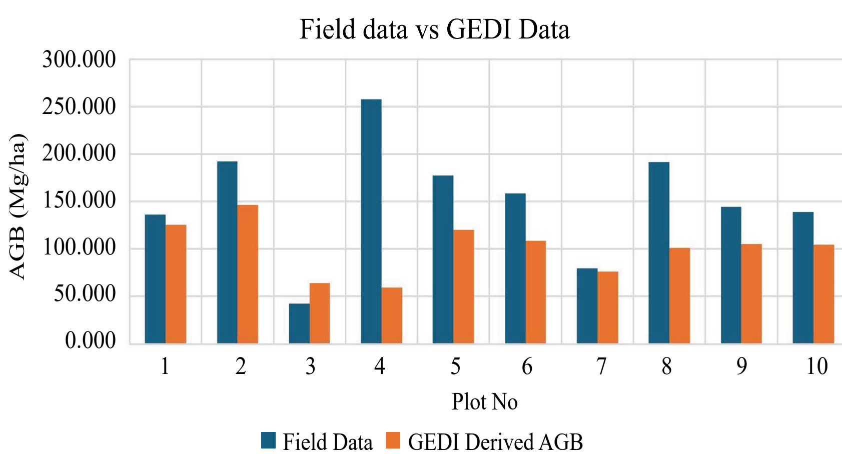

Figure 11. Comparison of field plot data (2025) vs GEDI-derived (2024) AGB. Bar chart comparing field-measured and GEDI-predicted AGB values across 10 sample plots, showing discrepancies and model performance.

environment and dominated by Swietenia Mahagoni, a species known for its high wood density and vertical growth. Such species-specific and site-specific attributes are often underrepresented in generalized remote sensing models, resulting in substantial underestimation.

Similar underpredictions are observed in other high-biomass plots such as Plots 2, 5, and 8. Conversely, in plots with lower observed AGB (e.g., Plots 3, 7, and 10), the predicted values align more closely with field data, indicating better model performance in low to moderate biomass ranges. These results suggest limitations in the model's capacity to account for species variation, urban planting structures, and irregular forest conditions.

To improve prediction accuracy, future modeling efforts should consider integrating species-specific parameters, higher-resolution spectral data, or structural metrics such as canopy height from LiDAR or GEDI sensors. This validation shows the importance of field calibration and highlights the potential biases when applying remote sensing models across heterogeneous landscapes.

Methodological limitations: The results can be influenced by multiple uncertainties associated with the biomass estimation procedure. These include methodological limitations such as sensor constraints (e.g., GEDI saturation in dense canopy), errors inherent in the regression modeling, and misclassification or spectral confusion of forest categories. Furthermore, it may be influenced by spatial mismatches resulting from geolocation errors, temporal differences between the GEDI and field data acquisition, and scaling errors. Therefore, while the final map offers valuable insight into spatial biomass dynamics, the results must be interpreted cautiously, acknowledging both the influence of environmental drivers and these methodological and sensor-related limitations.

Conclusion

This study showed that combining GEDI LiDAR and Sentinel-2 data can effectively track changes in above-ground biomass and carbon stock in Bhawal National Park. The results showed a clear drop in both AGB and carbon stock from 2019 to 2024. The estimated data moderately matched with field data, showing the model's reasonable accuracy. The maps revealed that most biomass loss happened near forest edges and areas affected by human activity. These losses are linked to deforestation, land conversion, and forest fragmentation. The overall trend highlights the growing pressure on the park's forest ecosystem, which threatens its long-term ecological balance and ability to act as a carbon sink. Forest degradation in Bhawal reflects broader environmental challenges in Bangladesh, where rapid urbanization and unplanned land use continue to reduce natural vegetation cover. Restoring degraded areas and promoting community-based forest management could help reverse this trend. Future work should focus on integrating higher-resolution LiDAR and hyperspectral data to improve model accuracy and better capture small-scale forest changes. Regular monitoring using GEDI and satellite data can support evidence-based decision-making for forest management, enhance national carbon accounting systems. Moreover, it will strengthen Bangladesh's role in achieving global climate goals through initiatives like REDD+.

References

Błońska E, Lasota J, Tullus A, Lutter R and Ostonen I. 2019. Impact of deadwood decomposition on soil organic carbon sequestration in estonian and polish forests. *Annals of Forest Science* 76.https://doi.org/10.1007/s13595-019-0889-9.

Breiman L. 2001. Random forests. Machine Learning, 45: 5-32.

Chamberlin A. J. 2025. A deep learning approach for High-Resolution canopy height mapping in Indonesian Borneo by fusing multi-source remote sensing data. Remote Sensing. 17: 3592. https://doi.org/10.3390/rs17213592.

Chave J, Andalo C, Brown S, Cairns MA, Chambers JQ, Eamus D, Fölster H, Fromard F, Higuchi N, Kira T, Lescure JP, Nelson BW, Ogawa H, Puig H, Riéra B and Yamakura T. 2005. Tree allometry and improved estimation of carbon stocks and balance in tropical forests. *Oecologia.* 145: 87-99. https://doi.org/10.1007/s00442-005-0100-x.

Chave J, Réjou-Méchain, Búrquez M, Chidumayo A, Colgan E, Delitti M. S., W. B. and Vieilledent, G. 2014. Improved allometric models to estimate the aboveground biomass of tropical trees. Global Change Biology. 20: 3177-3190. https://doi.org/10.1111/gcb.12629.

Delegido J., Verrelst J, Alonso L and Moreno J. 2011. Evaluation of Sentinel-2 red-edge bands for empirical estimation of green LAI and chlorophyll content. *Sensors*. 11: 7063-7081.

Dubayah R, Blair JB, Goetz S, Fatoyinbo L, Hansen M, Healey S, Hofton M, Hurtt G, Kellner J, Luthcke S, Armston J, Tang H, Duncanson L, Hancock S, Jantz P, Marselis S, Patterson PL, Qi W and Silva C. 2020. The Global ecosystem dynamics investigation: high-resolution laser ranging of the earth's forests and topography. Science of Remote Sensing. 1: 100002. https://doi.org/10.1016/j.srs.2020.100002.

Duncanson L, Kellner JR, Armston J, Dubayah R, Minor DM, Hancock S, Healey SP, Patterson PL, Saarela S, Marselis S, Silva CE, Bruening J, Goetz SJ, Tang H, Hofton M, Blair B, Luthcke S, Fatoyinbo L, Abernethy K, Zgraggen C. 2022. Aboveground biomass density models for NASA's Global Ecosystem Dynamics Investigation (GEDI) lidar mission. Remote Sensing of Environment. 270: 112845. https://doi.org/10.1016/j.rse.2021.112845.

Food and Agriculture Organization 2015. Global Forest Resources Assessment. 2015: How are the world's forests changing? *FAO*. https://www.fao.org/forest-resources-assessment.

Friedlingstein P, O'Sullivan M, Jones MW, Andrew RM, Hauck J, Landschützer P, Le Quéré C, Li H, Luijkx IT, Olsen A, Peters GP, Peters W, Pongratz J, Schwingshackl C, Sitch S, Canadell JG, Ciais P, Jackson RB, Alin SR, Zeng J. 2025. Global Carbon Budget 2024. Earth System Science Data. 17: 965-1039. https://doi.org/10.5194/essd-17-965-2025.

Gandhi U. 2024. Estimating Above-Ground Biomass using random forest regression in GEE: spatial thoughts. https://spatialthoughts.com/2024/02/07/agb-regression-gee/.

Harris NL, Gibbs DA, Baccini A, Birdsey RA, De Bruin S, Farina M, Fatoyinbo L, Hansen MC, Herold M, Houghton RA, Potapov PV, Suarez DR, Roman-Cuesta RM, Saatchi SS, Slay CM, Turubanova SA and Tyukavina A. 2021. Global maps of twenty-first-century forest carbon fluxes. *Nature Climate Change*. 11: 234-240. https://doi.org/10.1038/s41558-020-00976-6.

IPCC 2006. Guidelines for National Greenhouse Gas Inventories – A primer, Prepared by the National Greenhouse Gas Inventories Program: Eggleston HS, Miwa K, Srivastava N, Tanabe K (eds) Institute for Global Environmental Strategies, Japan.

Islam M, Deb GP and Rahman M. 2017. Forest fragmentation reduced carbon storage in a moist tropical forest in Bangladesh: Implications for policy development. *Land Use Policy*. 65:15-25. https://doi.org/10.1016/j.landusepol.2017.03.025.

Jahan I, Thompson PM, Paul E, Sultana N, Roy K and Mallick A. 2017. Birds of Bhawal National Park, *Bangladesh. Forktail*. 33: 88-91

Kabir DS and Ahmed AZ. 2005. Wildlife biodiversity in Bhawal National Park: Management techniques and drawbacks. *Our Nature.* 3: 83-90.

Lu D. 2006. The potential and challenge of remote sensing–based biomass estimation. *International Journal of Remote Sensing*. 27: 1297-1328.

Mojumder A, Hossain MS and Volk TA. 2023. Estimation of aboveground forest biomass and carbon storage of Bangladesh. *BIOTROPIA*, 30: 263-281. https://doi.org/10.11598/btb.2023.30.3.1858.

Muhe S. and Argaw M. 2022. Estimation of Above-Ground Biomass in Tropical Afro-Montane Forest Using Sentinel-2 Derived Indices. *ENVIRONMENTAL SYSTEMS RESEARCH*. https://doi.org/10.1186/s40068-022-00250-y.

Nuthammachot N, Askar A, Stratoulias D and Wicaksono P. 2020. Combined use of Sentinel-1 and Sentinel-2 data for improving above-ground biomass estimation. *Geocarto International*. 37: 366-376. https://doi.org/10.1080/10106049.2020.1726507.

Pan Y, Richard A. Birdsey, Jingyun Fang, Richard Houghton, Pekka E. Kauppi, Werner A. Kurz, Oliver L. Phillips, Anatoly Shvidenko, Simon L. Lewis, Josep G. Canadell, Philippe Ciais, Robert B. Jackson, Stephen W. Pacala, A. David Mcguire, Shilong Piao, Aapo Rautiainen, Stephen Sitch, And Daniel Hayes. 2011. A Large And Persistent Carbon Sink in the World's Forests, Science. 333: 988-993. https://doi.org/10.1126/science.1201609.

Rahman MU, Dey T and Biswas J. 2023. Land-use change and forest cover depletion in Bhawal National Park, Gazipur, Bangladesh from 2005 to 2020. *Environmental Monitoring and Assessment*. 195. https://doi.org/10.1007/s10661-022-10764-8.

Wijas Baptiste J, Steven D, Allison AT, Austin WK, Cornwell J, Hans C, Cornelissen PE, Shawn F, Mark KJ, Ooi JR, Powell C, Woodall W and Amy EZ. 2024. The Role of Deadwood in the Carbon Cycle: Implications for Models, Forest Management, and Future Climates. *Annual Review of Ecology Evolution and Systematics* 55: 133–55. https://doi.org/10.1146/annurev-ecolsys-110421-102327.

Xie Y, Sha Z and Yu M. 2008. Remote sensing imagery in vegetation mapping: A review. *Journal of Plant Ecology*. 1: 9-23.

Zanne AE, Lopez-Gonzalez G, Coomes DA, Ilic J, Jansen S, Lewis SL, Miller RB, Swenson NG, Wiemann MC and Chave J. 2009. Global wood density database. Dryad. Identifier: http://hdl.handle.net/10255/dryad.235.

Zhang X, Ni-meister W. 2014. Remote Sensing of Forest Biomass. In: Hanes J. (eds) Biophysical Applications of Satellite Remote Sensing. Springer Remote Sensing/Photogrammetry. Springer, Berlin, Heidelberg. Pp. 63-98. https://doi.org/10.1007/978-3-642-25047-7_3.